Available online at www.sciencedirect.com
ScienceDirect
Computers and Mathematics with Applications 53 (2007) 209–218
An International Journal
computers & mathematics
with applications
www.elsevier.com/locate/camwa

Implicit constitutive equations in the modeling of bimodular materials: An application to biomaterials

Francesco Mollica[a,*], Maurizio Ventre[b], Fernando Sarracino[b], Luigi Ambrosio[b], Luigi Nicolais[b]

[a] *Department of Engineering, Università di Ferrara, Via Saragat 1, 44100 Ferrara, Italy*
[b] *IMCB – Institute for Composite and Biomedical Materials, National Research Council, P. le Tecchio 80, 80125, Napoli, Italy*

Received 13 September 2005; accepted 27 February 2006

Abstract

Hyaff 11®, a material derived from hyaluronic acid with interesting applications as a scaffold for tissue engineering, is made porous by salt leaching and mechanically tested in simple tension and confined compression. The tests revealed a different behavior in tension and compression, a feature common to other foamed materials. The difference between the behavior in tension and compression is such that the material cannot be modeled with a traditional constitutive law, thus an implicit constitutive equation valid for finite deformations is formulated, and a suitable selectivity criterion is proposed in order to distinguish the behavior in tension from that in compression. The results of the model are compared with the experimental findings both in simple tension and in confined compression, yielding a good fitting with five material parameters.

Keywords: Implicit constitutive equations; Foam modeling; Biomaterials; Continuum Mechanics

1. Introduction

In the field of biomaterials there is an increasing need for materials that are biocompatible and resorbable, i.e. that can progressively degrade after implantation, releasing degradation products that can enter the normal metabolic pathways. Such materials can be used in a variety of ways; for example they can serve as scaffold for tissue engineering applications [1], i.e. a supporting framework mimicking the natural tissue extra cellular matrix (ECM), onto which cells can attach, proliferate and differentiate, in order to synthesize a tissue or an organ. Resorbability is conveniently exploited in such an application, as the material can be made to be resorbed by the body once the tissue or organ is completely formed. Synthetic bioresorbable polymers, like polyglycolyc acid (PGA), poly-L-lactic acid (PLLA), polyvinylalcohol (PVA) and polycaprolactone (PCL), have been widely used in biomaterial production, owing to their good mechanical properties, biocompatibility and consistency in production. New resorbable materials, produced starting from natural components, are entering the market thanks to their very

* Corresponding author.
E-mail address: francesco.mollica@unife.it (F. Mollica).

0898-1221/$ - see front matter © 2007 Elsevier Ltd. All rights reserved.
doi:10.1016/j.camwa.2006.02.020

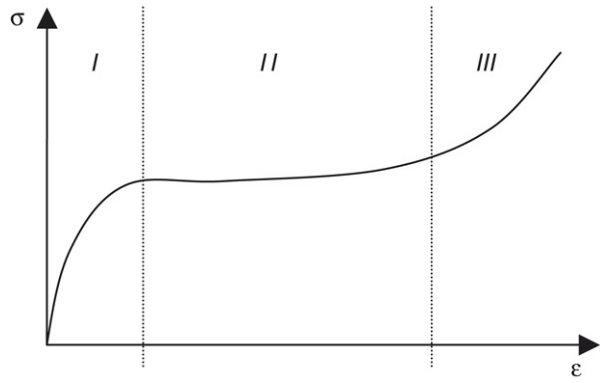

Fig. 1. A generic stress–strain curve for a foam in compression displaying the three typical regions.

interesting properties. Such materials, indeed, possess information and signaling properties within their structure (peptide and polysaccharide sequences, hydrophobic and hydrophilic patches, etc.), which can trigger important biological events at the cellular level. One of these materials is Hyaff®, which is derived from hyaluronic acid, a member of the glycosaminoglycan family. Hyaluronic acid, also termed hyaluronan, is present in a wide variety of vertebrate tissues [2], contributing to morphogenesis, tissue remodeling and inflammatory events [3–5]. Esterification of hyaluronic acid produces a material that has interesting mechanical properties [6,7] and can be conveniently used in the treatment of osteoarthritis [8], burn covering grafts [9] and in tissue engineering [10].

The tissue engineering scaffold has to have primarily good properties of biocompatibility and permeability to fluids that supply nutrients to the cells. This is one of the reasons why scaffolds are usually porous materials, with interconnected porosity [11]. Pore size is in fact a very important factor in the realization of a successful scaffold. Nevertheless, mechanical properties also have to be adequate to withstand the loads applied after implantation. It is well known [12] that the behavior of cells in terms of their proliferation, differentiation and overall well-being is profoundly influenced by the mechanical environment they are immersed in: in the case of a tissue engineering scaffold such an environment is created by the external forces that are transmitted to the cells through the scaffold. In order to gain an accurate knowledge of such forces, it is necessary to have a constitutive equation for the material of which the scaffold is made, valid both in tension and compression, and capable of accurately modeling the behavior also in the case of large deformations, as the material is usually very compliant.

The modeling of porous materials is often based on the mechanics of cellular materials [13]: the material is assumed to be composed of a regular array of elementary cells, whose deformation can be studied with the help of known theories, such as linear elasticity, applied to the struts or plates that make up the elementary cell. Such an approach has produced a number of interesting results [14], due to the great resemblance between foams and the idealized cellular material, but also has a few drawbacks. For instance, the results obtained depend on the shape of the elementary cell that is chosen, real materials are not necessarily made of equal repeated elementary cells, solving problems numerically generally requires relatively long computing times, and the solution of problems with large compressive deformations becomes particularly complicated due to issues of contact among the parts of the elementary cells: at large deformations the cell structure collapses completely increasing the apparent density of the material and making the struts and plates of every cell contact each other [15].

Some of these problems could be avoided by using a model formulated within the context of continuum mechanics, but to find such a model is still an open problem. In particular, one issue to be solved is the different mechanical response of the material in tension and compression. Let us consider a flexible foam subject to large deformations: when the cellular structured material is in tension the struts and plates composing the cells respond by progressively aligning themselves along the traction direction. In compression, on the other hand, after a first small region in which the struts and plates are being compressed, once a critical load has been reached they buckle giving way to a plateau region in which the stress–strain curve of the material has almost zero slope. In this region, the apparent density of the material grows until the stress–strain curve increases again (third region) until failure or total collapse of the cellular structure (Fig. 1). It is thus clear that foamed materials behave very differently in tension and compression.

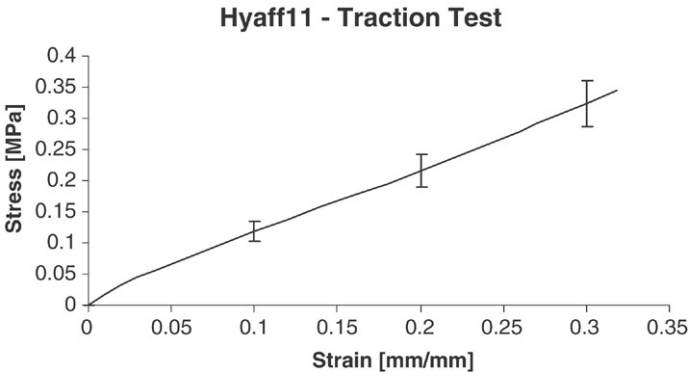

Fig. 2. Stress–strain relationship in tension for Hyaff 11: average curve. The error bars denote the standard deviation.

Many materials are known to display different properties in tension and compression. Fiber reinforced composites [16], brittle materials with damage [17] and biological materials such as cartilage [18] can be taken as examples. Conewise Linear Elasticity, formulated by Curnier et al. [19], is a constitutive law suitable for modeling elastic materials presenting a different behavior in tension and compression and has been successfully applied to cartilage [20,21]. On the other hand, since such a model is based on linear elasticity, its application is restricted to cases of small deformations, and this is too limiting a condition for materials like the one considered in this work. A generalization, which is valid in the case of finite deformations, can be sought using the notion of implicit constitutive laws. This concept is not new in continuum mechanics [22], and it has already been applied to many different fields, such as fluids with pressure dependent viscosity [23] and plastically deforming solids [24], but it has been fully exploited only quite recently by Rajagopal [25,26].

The aim of the present paper is hence to find a suitable implicit constitutive equation that can model materials that have different behavior in tension and compression without being limited to small strains. In the next section the experiments performed on the benzylic ester of hyaluronan are described and the results are presented. In Section 3 it will be explained why, based on the experimental work, it is not possible to find an explicit constitutive equation for the material under examination. Implicit constitutive equations and the applications to solid mechanics are briefly reviewed in Section 4 and a specific form applied to the case of the present paper is described in Section 5. In Section 6 the results of the model are compared with the experimental findings and discussed.

2. Experimental

The material under study is the benzylic ester of hyaluronic acid (Hyaff 11®, Fidia Advanced Biopolymers, Italy). In order to characterize such a material in tension, it was first dissolved in dimethylsulfoxide (DMSO, Sigma Aldrich, MO, USA) 8/92 wt. A solution of 4% wt of polyethylene glycol 400 (PEG400, Fluka, Buchs, Switzerland) was added as a plasticizing agent. Sodium chloride 99.5% purity grade (Ashland Chemicals, OH, USA) was also added to the solution as a porosity inducing agent. The salt was mechanically sieved in order to obtain particles having dimensions in the range of 300–500 μm. The polymer/salt weight ratio was kept at the constant value of 15/85.

The polymer solution was then poured onto 90 mm glass Petri dishes, obtaining discs with a uniform 3 mm thickness. In order to extract the solvent the dishes were soaked in a solution of ethanol 96% (J.T. Baker, Phillipsburg, NJ, USA) and PEG400 75/25 vol. The ethanol/PEG solution was changed every 24 hours for 7 days. Afterwards, the discs were immersed into a solution of bidistilled water and PEG400 75/25 vol. The immersion in aqueous solution caused the salt to dissolve, thus yielding a porous material. The water/PEG solution was changed every 24 hours for 7 days. Six wet specimens, shaped according to the ASTM 1708 standard, having a thickness of 1.48 ± 0.24 mm, were punched from the discs. The specimens were then tested in simple tension on an INSTRON 4204 dynamometer (INSTRON Corporation, Canton MA, USA) at a crosshead speed of 1 mm/min at room temperature with a loading cell of 100 N. The displacement of the specimen was assumed to be equal to the displacement of the crosshead, since the specimen is much more compliant than the mobile parts of the dynamometer. The average stress–strain diagram is reported in Fig. 2.

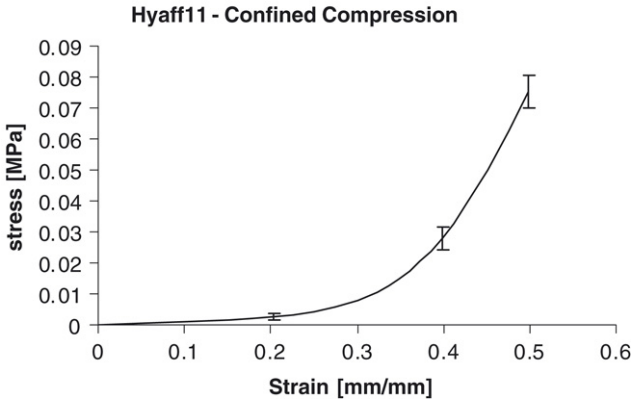

Fig. 3. Stress–strain relationship in confined compression for Hyaff 11. The error bars denote the standard deviation.

In order to complete the mechanical characterization, the material was also tested in confined compression. The Hyaff® porous film was prepared according to the same procedure described above. This time, though, the film was cut with a cylindrical socket puncher, obtaining eight discs having a diameter of 38 mm and a thickness of 6.55 ± 2.35 mm. Two overlapped wet samples were put in a stainless steel chamber (38 mm diameter) and covered by a stainless steel spacer. This spacer was drilled in several locations in order to let the water contained in the wet specimen escape through the holes during the compression testing. The specimens were then tested in confined compression on an INSTRON 4204 dynamometer at a crosshead speed of 1 mm/min at room temperature with a 100 N loading cell. The results in terms of the stress–strain diagram are shown in Fig. 3.

3. Modeling

Modeling a material with the response described by the graphs of Figs. 2 and 3 is a formidable task. In fact, as we can see from the figures, the slope of the curve (i.e. the stiffness) at small strains in confined compression is much smaller than the corresponding slope in simple tension. It is easy to show that there is no isotropic material that satisfies the requirement of having a higher stiffness in simple tension than in confined compression, as we shall see next.

Since strains can be assumed to be small in the limit for calculating the stiffnesses, we can consider a linear elastic isotropic material: the slope in simple tension is simply given by E, the Young's modulus of the material. In the case of confined compression, the slope instead is given by

$$K = \frac{E(1-\nu)}{(1-2\nu)(1+\nu)}, \tag{1}$$

where ν is Poisson's ratio, which has to satisfy the requirement $-1 < \nu < 0.5$. With this requirement, it is easy to show from (1) that K will always be greater than E. This leads to a constitutive law that has a different behavior in tension from that in compression. In fact, if we assume a different constitutive behavior between tension and compression (e.g. stiff in tension and compliant in compression) the graphs of Figs. 2 and 3 can be correctly fitted. Bimodular materials, i.e. materials that have different behavior in tension and compression, are not uncommon in nature. For instance, cartilage is well known to display this property [20], and anyway almost every material shows some differences when tested in tension and compression. The assumption of bimodularity for very flexible foams is not without a basis on physical grounds: open cell foamed materials have a cellular structure [13] characterized by an ordered arrangement of cells composed of strut- and plate-like elements. When these cells are subject to tension these elements respond by aligning themselves along the traction direction and the loads are borne by the material constituting the struts and plates that are mainly stretched. The mechanical response is thus quasi linear as in the case of the experiments that were described in the previous section. In compression, on the other hand, after the initial region in which the struts and platelets bear the applied load in compression, there is the plateau region where the struts and plates buckle. Hence, in this region the external applied load is carried mostly by the bending of the struts

and plates. It is thus clear that the behavior in compression has to be very different from the behavior in tension, so much so that we can think of modeling these behaviors as if they belonged to two distinct materials, in particular one that is stiff (in tension) and the other one that is compliant (in compression).

Comparing Figs. 1 and 3 we can see that the material we tested does not behave like a typical flexible foam in compression, since the first region is missing. One possible explanation is that problems in the experimental apparatus, e.g. alignment of the holding fixtures, have somehow cut the first region from the experiment. This is of course a problem, but on the other hand, since we are mainly interested in the behavior of the material at large deformations, and the first region is usually characterized by small loads and by a much smaller extension if compared to the plateau region, we can assume that the extension of the first region is so small that it can be assumed to be negligible with respect to the extension of the plateau region. In such a case the behavior in compression is given by the plot of Fig. 2, without making a significant error.

Implicit constitutive equations can provide a useful tool to mathematically treat materials that have different behavior in tension and compression, as we shall see in the next sections.

4. Implicit constitutive equations

For the case of solid mechanics implicit constitutive laws were investigated by Rajagopal and Wineman [23] to model the behavior of materials that can have multiplicity of responses from a branch point. For the sake of clarity we will briefly review the main points of the work of Rajagopal and Wineman for the one-dimensional case. The constitutive equation is given as an implicit function of σ and ε as follows:

$$F(\sigma, \varepsilon) = 0, \tag{2}$$

where σ denotes the stress and ε the linearized strain. A branch point is defined to be a point $(\sigma_0, \varepsilon_0)$ for which there exist at least two couples (σ, ε) that satisfy (2) at $(\sigma_0, \varepsilon_0)$. Further, if there exist closed balls $C_i \subset \Re$ which contain ε_0, and there exist differentiable functions $g_i : C_i \to \Re$ such that $(g_i(\varepsilon), \varepsilon)$ solves (2), then $g_i(\varepsilon)$ is a branch of F at ε_0. Note that at a branch point there must be at least two branches. The effective behavior of the material is given by the response function $\phi(\varepsilon)$, which has the following properties: (i) $[\phi(\varepsilon), \varepsilon]$ satisfies (2); (ii) $\mathrm{d}\phi/\mathrm{d}\varepsilon \geq 0$; (iii) at any branch point $(\sigma_0, \varepsilon_0)$ the response function equals one of the branches which is chosen by a suitable selectivity condition.

As an example, for the case of a strain hardening elastic plastic material, their analysis led to the following constitutive equation:

$$F(\sigma, \varepsilon) = [\sigma - E\varepsilon]\left[\frac{\varepsilon_1}{U}(\sigma - E\varepsilon) + (\varepsilon - \varepsilon_1)\right]\left[\frac{\varepsilon_1}{U}(\sigma - E\varepsilon) + (\varepsilon + \varepsilon_1)\right] = 0, \tag{3}$$

in which the first factor models the elastic response, while the other two approximate the strain hardening parts in tension and compression. The meaning of the symbols in (3) is as follows: E is the Young's modulus of the material, ε_1 is the yield strain (supposed to be equal in tension and compression) and U is a material constant related to the slope of the stress–strain diagram after yielding, i.e. the strain hardening part. The selectivity condition used in this case is as follows:

$$\phi(\varepsilon) = \begin{cases} g_L(\varepsilon) & \text{if } \phi(\varepsilon_0)\mathrm{d}\varepsilon > 0 \\ g_U(\varepsilon) & \text{if } \phi(\varepsilon_0)\mathrm{d}\varepsilon \leq 0 \end{cases} \tag{4}$$

with

$$\begin{aligned} \frac{\mathrm{d}g_L}{\mathrm{d}\varepsilon} &\leq \frac{\mathrm{d}g_i}{\mathrm{d}\varepsilon} \\ \frac{\mathrm{d}g_U}{\mathrm{d}\varepsilon} &\geq \frac{\mathrm{d}g_i}{\mathrm{d}\varepsilon} \end{aligned} \qquad \forall g_i,\ i = 1 \ldots n,$$

which implied that the chosen branch was the one that minimized the increment in expended energy on loading and maximized the increment of recovered energy on unloading. Such a condition, of course, is specific for this application and need not apply to all materials.

The approach of implicit constitutive equations can be conveniently exploited in the case of a material having a different response in tension and compression. Let us consider first for simplicity the one-dimensional case. If we

denote by f_t and f_c the mechanical responses in tension and compression, respectively, we can incorporate both functions in the same implicit constitutive law as follows [27]:

$$F(\sigma, \varepsilon) = [\sigma - f_t(\varepsilon)][\sigma - f_c(\varepsilon)] = 0, \tag{5}$$

where σ and ε have the same meaning as in (2). Clearly (0, 0) will be a branch point for the material; the two responses f_t and f_c can be taken in such a way that this is the only one. As far as the selectivity condition is concerned, a convenient criterion may be one that selects the branch at (0, 0) directly on the basis of the stiffness: if the material is stiffer in tension than in compression, as in the case of Hyaff®, then a convenient choice can be

$$\phi(\varepsilon) = \begin{cases} f_t(\varepsilon) & \text{if } \mathrm{d}\varepsilon > 0 \text{ (tension)} \\ f_c(\varepsilon) & \text{if } \mathrm{d}\varepsilon \leq 0 \text{ (compression)} \end{cases} \tag{6}$$

where f_t and f_c are branches at (0, 0) such that

$$\begin{aligned} \frac{\mathrm{d}f_t}{\mathrm{d}\varepsilon} &\geq \frac{\mathrm{d}g_i}{\mathrm{d}\varepsilon} \\ \frac{\mathrm{d}f_c}{\mathrm{d}\varepsilon} &\leq \frac{\mathrm{d}g_i}{\mathrm{d}\varepsilon} \end{aligned} \qquad \forall g_i,\ i = 1 \ldots n,\ \text{branches of } F \text{ at } (0, 0). \tag{7}$$

A possible generalization of the above approach to the three-dimensional case, together with an application to hyaluronic acid will be described in the next section.

5. Specific form

For the three-dimensional case, let the position of a generic particle of the material in the reference configuration be represented by $\mathbf{X}$, and let $\mathbf{x}(t)$ be the position of the same particle in the current configuration at time t. As usual, we will indicate the motion by $\mathbf{x} = \chi(\mathbf{X}, t)$, while the deformation gradient $\mathbf{F}$ is obtained from

$$\mathbf{F}(\mathbf{X}, t) = \frac{\partial \chi(\mathbf{X}, t)}{\partial \mathbf{X}}, \tag{8}$$

and is an invertible tensor, i.e. $J = \det \mathbf{F} > 0$. Using polar decomposition we have $\mathbf{F} = \mathbf{RU} = \mathbf{VR}$, where $\mathbf{R}$ is a proper orthogonal tensor and $\mathbf{U}$ and $\mathbf{V}$ are the left and right stretch tensors, respectively. We will indicate by λ_1, λ_2 and λ_3 the principal stretches, i.e. the eigenvalues of the stretch tensors, so that $J = \lambda_1\lambda_2\lambda_3$.

We will write the implicit constitutive equation in terms of the principal stresses and principal stretches. Using the hypothesis of isotropy, the principal directions of stress and stretch coincide. Such a hypothesis is not usually true for materials that are foamed with physical or chemical expanding agents, since the expansion usually occurs in a particular direction yielding pores elongated in that direction and thus leading to a transversely isotropic material. In our case, though, porosity was obtained by salt leaching; thus we can assume that the shape of the pores is almost not elongated. Instead, the material may not satisfy the assumption of homogeneity, since the salt will tend to settle on the bottom of the Petri dish, leaving in this location a higher void fraction with respect to the top. In order to reduce this phenomenon, the polymeric porous film was manufactured with a maximum thickness of 6–7 mm. In any case, for the sake of simplicity, at the modeling stage we will assume that the material be homogeneous and isotropic. In such a case, indicating the principal first Piola–Kirchhoff stresses by P_i, $i = 1, 2, 3$, we will assume:

$$F(P_i, \lambda_1, \lambda_2, \lambda_3) = \left[P_i - \frac{\Phi}{\lambda_i}\left(\lambda_i^2 - \frac{1}{J^{2q}}\right)\right]\left[P_i - \frac{\Phi}{\lambda_i}\left(\lambda_i^2 - \frac{1}{J^{2q}}\right) - \frac{\Psi}{\lambda_i}\left(\lambda_i^m - \frac{1}{\lambda_i^n}\right)\right] = 0, \tag{9}$$

where Φ, Ψ, q, m and n are material constants. The first factor of (9) is designed to model the material response in compression, i.e. for $0 < \lambda_i < 1$, while the second factor will model the material response in tension, i.e. for $\lambda_i > 1$. The response of the material in compression is the same as for the "rigid polyurethane" described by Blatz and Ko [28], while the response in tension is a modified version of the same material that is stiffer if pulled in the i-th direction. The branch points of the material are at $P_i = 0$ and $\lambda_i = 1$; $\lambda_j = \lambda_k^{-1}$ with $i \neq j \neq k$. The branches at these points are identified by the two factors of (9). In order to choose the correct branch, one can use the selectivity

condition described in the previous section to correctly identify the response in compression from the one in tension:

$$P_i(\lambda_1,\lambda_2,\lambda_3)=\begin{cases} f_t^i(\lambda_1,\lambda_2,\lambda_3) & \text{if } \lambda_i > 1 \text{ (tension)} \\ f_c^i(\lambda_1,\lambda_2,\lambda_3) & \text{if } \lambda_i \le 1 \text{ (compression)} \end{cases} \tag{10}$$

with

$$\begin{aligned} \frac{\partial f_t^i}{\partial \lambda_i} &= \max\left[\left.\frac{\partial g}{\partial \lambda_i}\right| g \text{ branches of } F\,(P_i,\lambda_1,\lambda_2,\lambda_3)\right] \\ \frac{\partial f_c^i}{\partial \lambda_i} &= \min\left[\left.\frac{\partial g}{\partial \lambda_i}\right| g \text{ branches of } F\,(P_i,\lambda_1,\lambda_2,\lambda_3)\right]. \end{aligned} \tag{11}$$

Once this is done the constitutive equation reads:

$$\begin{cases} P_i = \dfrac{\Phi}{\lambda_i}\left(\lambda_i^2 - \dfrac{1}{J^{2q}}\right), & \text{if } 0<\lambda_i<1, \text{ (compression);} \\ P_i = \dfrac{\Phi}{\lambda_i}\left(\lambda_i^2 - \dfrac{1}{J^{2q}}\right) + \dfrac{\Psi}{\lambda_i}\left(\lambda_i^m - \dfrac{1}{\lambda_i^n}\right), & \text{if } \lambda_i>1, \text{ (tension),} \end{cases} \tag{12}$$

for each of the principal stresses, $i = 1, 2, 3$. Let us now apply this constitutive equation to the cases of confined compression and simple tension.

5.1. Confined compression

Let us consider an orthogonal reference frame. Assuming the material is being compressed along the third coordinate direction, the deformation gradient $\mathbf{F}$ reads:

$$\mathbf{F} = \operatorname{diag}[1, 1, \lambda_c], \tag{13}$$

where we have denoted by $\lambda_c < 1$ the compressive stretch. Since the deformation is homogeneous, the balance of linear momentum is trivially satisfied and we can obtain the three principal first Piola–Kirchhoff stresses directly from (12):

$$\begin{aligned} P_1 &= P_2 = \Phi\left(1 - \frac{1}{\lambda_c^{2q}}\right), \\ P_3 &= \frac{\Phi}{\lambda_c}\left(\lambda_c^2 - \frac{1}{\lambda_c^{2q}}\right). \end{aligned} \tag{14}$$

A plot of $(14)_2$ together with the experimental result for Hyaff® is depicted in Fig. 4. The material constants that have been used are $\Phi = 0.258$ kPa and $q = 4.36$.

5.2. Simple tension

Let us again consider an orthogonal reference frame and let us assume that the material is being pulled along the third coordinate direction. The deformation gradient in this case $\mathbf{F}$ reads:

$$\mathbf{F} = \operatorname{diag}[\lambda_t, \lambda_t, \lambda] \tag{15}$$

where λ is the longitudinal stretch and λ_t denotes the transverse stretch, supposed to be equal in both the directions orthogonal to the direction in which the force is applied. Again, since the deformation is homogeneous, the balance of linear momentum is trivially satisfied and the principal first Piola–Kirchhoff stresses can be written directly from (12):

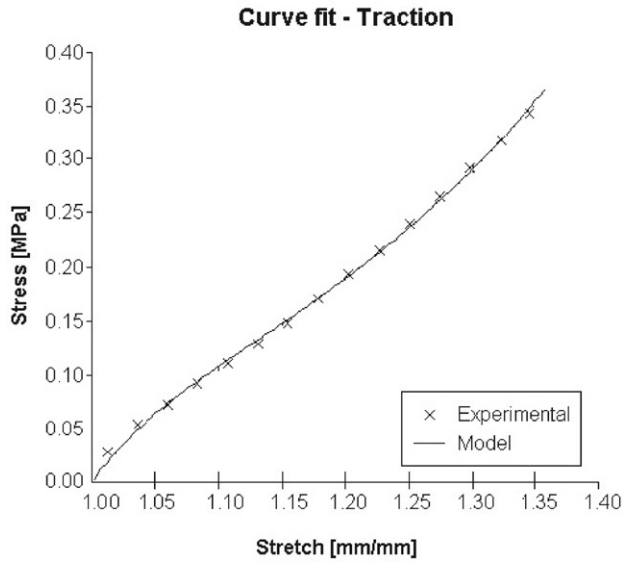

Fig. 4. Comparison model experiments in tension.

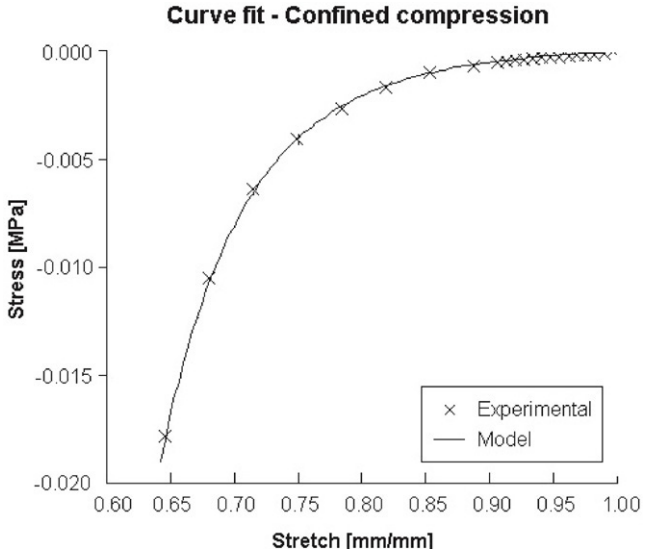

Fig. 5. Comparison model, experiment compression.

$$P_1 = P_2 = 0 = \frac{\Phi}{\lambda_t}\left(\lambda_t^2 - \frac{1}{\left(\lambda\lambda_t^2\right)^{2q}}\right),$$
$$P_3 = \frac{\Phi}{\lambda}\left(\lambda^2 - \lambda_t^2\right) + \frac{\Psi}{\lambda}\left(\lambda^m - \frac{1}{\lambda^n}\right). \tag{16}$$

The first equation superimposes that no forces are applied in the transverse direction, and is used to obtain the transverse stretch as a function of the longitudinal stretch. The second equation is then used to calculate the engineering stress and this result is compared with the experiments in Fig. 5. The material constants used are $\Phi = 0.258$ kPa, $q = 4.36$, as previously, and $\Psi = 74.7$ kPa, $m = 6.19$ and $n = 15.9$.

6. Discussion and conclusions

Porous Hyaff® 11 has been tested in simple tension and confined compression. The experimental curves that were obtained lead to a markedly different behavior in tension and compression, a feature common to many other materials such as cartilage. This has to be taken into account in the formulation of the model, which has also to be capable of describing the mechanical behavior of the material when subject to a general deformation history. In this sense it has been found to be convenient to formulate the constitutive law as an implicit equation, which contains both the response in tension and the one in compression, together with a selectivity condition that is used to choose the correct branch at branch points. Tension and compression are identified based on the principal stretches: it is assumed that a certain principal direction will be in tension if the corresponding principal stretch is greater than 1, the converse being true for compression. Although this seems to be the case on physical grounds, it does make things quite difficult, since for each general deformation, which the material will be subject to, one has to calculate at every instant and every location the eigenvalues and eigenvectors of stretch in order to tell the tension and compression direction and use the constitutive equation properly.

A different approach was followed by Curnier et al. [19], who identified tension and compression by checking the sign of the trace of the infinitesimal strain tensor. This has the great advantage of not requiring calculations of eigenvalues and eigendirections, with the drawback of being limited to small strains, since the whole model is based on linearized elasticity. Moreover, the physical meaning of the trace of the infinitesimal strain tensor is more connected to changes in volume rather than tension–compression differences, thus, a fortiori, the use of this model should be limited to the case of small strains where one may assume that a volume increase is related to tension and, conversely, a volume contraction to compression. In the limit of small strains, in fact, a cubic symmetric version of this model has been successfully applied to describe the mechanical behavior of cartilage [20].

As for the model presented in the present paper, the specific form described in the previous sections is able to approximate very well the mechanical behavior of Hyaff® in simple tension and in confined compression, for strains which are well above the limits considered as the threshold for large deformations. Overall the model requires five material constants, two of which are obtained from the experiment in confined compression and the remaining three from the experiment in simple tension. Although the deformations studied in this paper were limited to simple tension and confined compression for characterization purposes, the model can be used for more general deformations, such as inhomogeneous deformations.

The model that was developed in the present paper assumes that the material is elastic. This is in fact not true since one has to expect that the high water content renders the material viscoelastic. Moreover, the behavior in compression exhibits inelastic phenomena such as hysteresis and strain rate dependence (this behavior is not shown by the figures we presented in this paper), even in the case of a perfectly dry material. These features cannot be captured by the model described by (9); a generalization of it is currently under study.

Acknowledgement

The financial support by “Fondo Speciale per lo Sviluppo della Ricerca di Interesse Strategico” is gratefully acknowledged.

References

[1] B.D. Ratner, A.S. Hoffman, F.J. Schoen, J.E. Lemons, Biomaterials Science, Associated Press, 1996.
[2] J.R. Fraser, T.C. Laurent, U.B. Laurent, Hyaluronan: Its nature, distribution, functions and turnover, J. Intern. Med. 242 (1997) 27–33.
[3] B.P. Toole, Hyaluronan in morphgenesis, Cell Dev. Biol. 12 (2001) 79–87.
[4] B.P. Toole, in: R.V. Iozzo (Ed.), Hyaluronan in Proteoglycans: Structure Biology and Molecular Interaction, Marcel Dekker, New York, 2000, pp. 61–92.
[5] T.C. Laurent, The Chemistry, Biology and Medical Applications of Hyaluronan and its Derivatives, Portland Press, London, 1998.
[6] M. Mensitieri, L. Ambrosio, L. Nicolais, D. Bellini, M. O’Regan, Viscoelastic properties modulation of a novel autocrosslinked hyaluronic acid polymer, J. Mater. Sci.: Mater. Med. 7 (1996) 695–698.
[7] S. Iannace, L. Ambrosio, L. Nicolais, A. Rastrelli, A. Pastorello, Thermomechanical properties of hyaluronic acid derived products, J. Mater. Sci.: Mater. Med. 3 (1992) 59–64.
[8] R. Barbucci, S. Lamponi, A. Borzacchiello, L. Ambrosio, M. Fini, P. Torricelli, R. Giardino, Hyaluronic acid hydrogel in the treatment of osteoarthritis, Biomaterials 23 (2002) 4503–4513.

[9] H.S. Yoo, E.A. Lee, J.J. Yoon, T.G. Park, Hyaluronic acid modified biodegradable scaffolds for cartilage tissue engineering, Biomaterials 26 (2005) 1925–1933.
[10] D. Campoccia, P. Doherty, M. Radice, P. Brun, G. Abatangelo, D.F. Williams, Semisynthetic resorbable materials from hyaluronan esterification, Biomaterials 19 (1998) 2101–2127.
[11] T.M. Freyman, I.V. Yannas, L.J. Gibson, Cellular materials as porous scaffolds for tissue engineering, Progr. Mater. Sci. 46 (2001) 273–282.
[12] M. Chiquet, A.S. Renedo, F. Huber, M. Flück, How do fibroblasts translate mechanical signals into changes in extracellular matrix production? Matrix Biol. 22 (2003) 73–80.
[13] L. Gibson, M.F. Ashby, Cellular Solids. Structure and Properties, Cambridge University Press, 2001.
[14] L. Gong, S. Kyriakides, W.Y. Jang, Compressive response of open cell foams. Part I: Morphology and elastic properties, Internat. J. Solids Structures 42 (2005) 1355–1379.
[15] S.G. Bardenhagen, A.D. Brydon, J.E. Guilkey, Insight into the physics of foam densification via numerical simulation, J. Mech. Phys. Solids 53 (2005) 597–617.
[16] R.M. Jones, Stress–strain relations for materials with different moduli in tension and compression, AIAA J. 15 (1977) 16–23.
[17] H. Horii, S. Nemat-Nasser, Overall moduli of solids with microcracks-load-induced anisotropy, J. Mech. Phys. Solids 31 (1983) 155–171.
[18] V.C. Mow, X.E. Guo, Mechano-electrochemical properties of articular cartilage: Their inhomogeneities and anisotropies, Annu. Rev. Biomed. Eng. 4 (2002) 175–209.
[19] A. Curnier, Q.C. He, P. Zysset, Conewise linear elastic materials, J. Elasticity 37 (1995) 1–38.
[20] M.A. Soltz, G.A. Ateshian, A conewise linear elasticity mixture model for the analysis of tension-compression nonlinearity in articular cartilage, ASME J. Biomech. Eng. 122 (2000) 576–586.
[21] C.Y. Huang, A. Stankiewicz, G.A. Ateshian, V.C. Mow, Anisotropy, inhomogeneity, and tension-compression nonlinearity of human glenohumeral cartilage in finite deformation, J. Biomech. 38 (2005) 799–809.
[22] A.J.A. Morgan, Some properties of media by constitutive equations in implicit form, Int. J. Eng. Sci. 4 (1966) 155–160.
[23] J. Hron, J. Malek, K.R. Rajagopal, Simple flows of fluids with pressure-dependent viscosities, Proc. R. Soc. Lond. A457 (2001) 1603–1622.
[24] K.R. Rajagopal, A. Wineman, On constitutive equations for branching of response with selectivity, Int. J. Non Lin. Mech. 15 (1980) 83–91.
[25] K.R. Rajagopal, Implicit constitutive equations in engineering science, in: SES 41st Annual Technical Meeting, Lincoln, Nebraska, Oct. 11–13, 2004.
[26] K.R. Rajagopal, On implicit constitutive theories for fluids, J. Fluid Mech. 550 (2006) 243–249.
[27] K.R. Rajagopal, Private communication (2005).
[28] P.J. Blatz, W.L. Ko, Application of finite elasticity theory to the deformation of rubbery materials, Trans. Soc. Rheol. 6 (1962) 223–251.